Desalination and Water Treatment
www.deswater.com

doi: 10.1080/19443994.2016.1145603

57 (2016) 25226–25234
November

Taylor & Francis
Taylor & Francis Group

Synthesis and characterization of cobalt phthalocyanine/MCM-41 and its photocatalytic activity on methyl orange under visible light

Dejun Wang, Rui Guo, Shuaijun Wang, Fang Liu*, Yongqiang Wang, Chaocheng Zhao*

College of Chemical Engineering, China University of Petroleum (East China), Qingdao 266580, China, Tel. +86 53286981719; emails: wdjhello@163.com (D. Wang), 510723689@qq.com (R. Guo), 1055439500@qq.com (S. Wang), Tel. +86 53286984668; email: liufangfw@upc.edu.cn (F. Liu), Tel. +86 53286984680; email: wangyq@upc.edu.cn (Y. Wang), Tel. +86 53286981719; email: zhaochch@upc.edu.cn (C. Zhao)

Received 4 September 2015; Accepted 14 January 2016

ABSTRACT

The photocatalytic activity of cobalt phthalocyanine (CoPc) immobilized onto MCM-41 was investigated for decomposition of methyl orange in aqueous solutions. The morphology and structure of the catalyst were analyzed by diffuse reflectance ultraviolet-visible (DR UV–vis), X-ray diffraction, Fourier transform infrared, and scanning electron microscopy (SEM). Photocatalytic efficiency of the prepared catalyst for degradation of methyl orange was tested under illumination of visible light. The photodegradation process is completed within 2 h using a dose of 0.04 g/L of the catalyst in the 0.05 g/L of methyl orange solution under Xenon lamp, and the removal rate was 98.3%. The obtained results revealed that the photocatalyst was very active in degradation of methyl orange.

Keywords: CoPc; MCM-41; Degradation; Methyl orange; Photocatalysis

1. Introduction

Nowadays, water environment pollution has become a common concern in the world, especially, organic pollutants produced by some industries are harmful to human health and living creatures. The growing pollution of our hydrosphere has stimulated the need for developing new technologies for water and wastewater treatment [1].

Owing to the urgent need for a clean and comfortable environment, photocatalysis technique offers great potential for the elimination of toxic chemicals in the environment through its efficiency and broad applicability [2,3]. So far, many experts have done lots of researches on photocatalysis degradation, which mainly concentrated on semiconductor under UV irradiation, such as TiO_2 [4], ZnO [5], CdS [6], tungsten oxide [7], bismuth complex oxides [8]. Unfortunately, only a very small fraction (3–5%) of the solar spectrum falls in the UV region [9–11].

Phthalocyanine compound was first observed by Professor A. Braun and Professor T.C. Tcherniac in 1907, since then many studies have been conducted on its photocatalytic degradation of refractory pollutants in sewage. Metal phthalocyanine (MPc), a most promising photocatalyst with extraordinary molecular stability, negligible toxicity, and relatively simple preparation in a large scale has attracted considerable interest in recent years for the intense absorption bands in the longer wavelength region of the visible light in a solar spectrum. However, this application is

*Corresponding authors.

restricted by the difficulty in recovery and high tendency for aggregation of planar macrocycles [12], which impair the catalytic activity [13]. For this purpose, some strategies have been used to support catalysts onto different materials. In some cases resin [14] or naturally occurring minerals, such as bentonite [15], have been used; in addition, phthalocyanines have been hosted onto fiber [16] or mesoporous titanium dioxide [17]. Nonetheless, in most cases, zeolites [18] have been employed as supports following different experimental procedures for incorporation of phthalocyanines. Thus, phthalocyanines has been included within extralarge pore zeolitic aluminosilicates, such as MCM-41 [19]. These materials provide an adequate balance between moderate cage effect and facilitation of molecular traffic through the mesopores [20]. As the diameter of the channels (2 nm) allows diffusion of phthalocyanines, a simple ion-exchange procedure can be employed to incorporate this organic compound.

In the present work, we have carried out anchorage of CoPc with the aid of N–N dimethyl-formamide (DMF) to the wall of MCM-41. The resulting solid product was characterized by UV–vis, X-ray diffraction (XRD), Fourier transform infrared (FT-IR), and SEM techniques. Laboratory-scale batch experiments were conducted to investigate the degradation of methyl orange under visible light irradiation using the synthesized CoPc as photocatalyst. The influence of irradiation, immobilization, and amount of the catalyst on the degradation rate has been investigated.

2. Material and methods

2.1. Materials and reagents

Cobalt chloride, phthalic anhydride, urea, ammonium molybdate, N–N dimethylformamide (DMF) were of AR grade, obtained from Sinopharm Chemical Reagent Company, China and were used as received. All other reagents used were of analytical grade and were used as such without purification, unless otherwise mentioned. The commercial MCM-41 (LiYuan Co., Shandong, China) with an average pore size of 3.6 nm and specific surface area of 1,000 m^2/g was used after reactivation.

2.2. Preparation of CoPc/MCM-41

2.2.1. Synthesis of CoPc

Cobalt phthalocyanine (CoPc) was synthesized by modifying slightly the procedure described for the synthesis of other metal phthalocyanines [21,22]. A total of 7.4 g (50 mmol) phthalic anhydride, 1.363 g (10 mmol) cobalt chloride, 15.015 g (50 mmol) urea, and 0.148 g (0.76 mmol) ammonium molybdate were mixed well and heated slowly under reflux to 140˚C while stirring over an oil bath, at which point the phthalonitrile melts and forms a black blue slurry. The reaction mixture was then heated to 190˚C and maintained at 190˚C for 2 h with constant stirring. The crude product was cooled to room temperature and the solid mass was finely ground and washed with HCl solution (2%), NaOH solution (5%), and distilled water alternately to remove the intermediates and unreacted components until the filtrate was neutral. The product was dried in the oven for 12 h to obtain 4.3 g of a black-blue solid.

2.2.2. Preparation of loaded catalyst

In a typical reaction, 0.05 g of CoPc was added to a suspension of 0.5 g calcined MCM-41 in 20-mL DMF. The mixture was stirred for 20 min at room temperature and treated by ultrasonic dispersion for 20 min. The solution was separated by filtration, washed with DMF until it turns colorless. Finally, the solid product was dried at 100˚C for 6 h. This compound is called CoPc/MCM-41.

2.3. Characterization

The UV–vis spectroscopy of the sample was recorded on a TU-1901 spectrophotometer (Pgeneral, China), the scan range was 300–800 nm. XRD was performed on a panalytical X'pert PROX-ray diffractometer with Cu Kα monochromatized radiation (λ = 1.54 Å) operated at 45 kV and 40 mA. The scan rate was 8˚/min and the 2θ scan range was from 1.5˚ to 10˚. Morphological information was collected on a FEI Quanta200 scanning electron microscope (SEM) instrument. FT-IR spectrum was collected on a Nexus spectrometer (Nicolet, USA) in the range of 4,000–400 cm^{-1} with 32 scans and the samples were prepared as KBr pellets.

2.4. Photocatalytic decomposition monitoring

The schematic diagram of the photocatalytic reactor was shown in Fig. 1. The experiments for methyl orange photodegradation were carried out using a Model XPA-2 photocatalytic reactor (Xujiang Electrochemical Plant, Nanjing, China). A 1,000 W xenon lamp placed in a quartz socket tube with one end closed was used as the light source. Air was bubbled through the reaction solution from the bottom with an air flow of 0.5 L/min to ensure effective dispersion

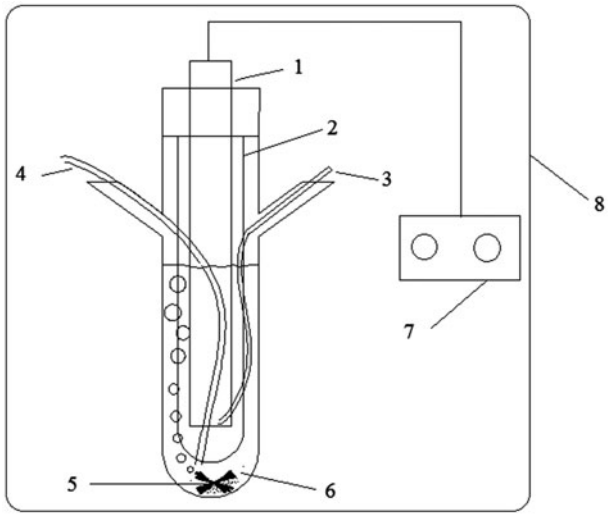

Fig. 1. The schematic diagram of the photocatalytic reactor. Notes: (1) xenon lamp; (2) quartz socket tube; (3) sampling port; (4) air inlet; (5) stirrer; (6) CoPc/MCM-41; (7) light controller; (8) dark room.

and a constant dissolved O_2 concentration. The temperature inside the reactor was maintained at 25˚C by means of a continuous circulation of water.

A total of 200.0 mL of the methyl orange solution (0.05 g/L) with proper catalyst poured into the reactor prior to each run. Before this, the solution was stirred in the dark for 1 h to obtain a good dispersion and established adsorption–desorption equilibrium between the organic molecules and the catalyst surface. Take a sample every 20 min and 15 mL every time. The samples were centrifuged and the supernatant was analyzed. Decreases in the concentrations of dyes were analyzed by a TU-1901 UV–vis spectrophotometer at 464 nm. At given intervals of illumination, the samples of the reaction solution were taken out and analyzed. The degradation efficiency of the as-prepared samples was defined as Eq. (1) [23]:

$$D_{\text{removal}} = (D_0 - D_t)/D_0 \times 100\% \quad (1)$$

where D_{removal} is the degradation efficiency, D_0 is the initial absorbance of methyl orange solution, and D_t is the absorbance of the treated solution after photocatalysis time t (min), respectively. All tests were conducted in triplicate.

3. Results and discussion

3.1. Characterization of the catalyst

Structural characteristics of the solid materials are listed in Table 1. A decrease in specific surface area from 1,060 to 630 m^2/g corresponding to a decrease in the pore volume from 0.97 to 0.56 cm^3/g may indicate a successful anchorage of CoPc to the walls of MCM-41. The BET specific surface area of the catalyst was evaluated and it was 630 m^2/g. Therefore, there is enough space for oxidizing the organic compounds via formation of active species.

The UV–vis absorption spectrum is an excellent tool for phthalocyanine investigation and characterization. The spectra of the phthalocyanine system exhibit characteristic Q and B bands [24–26]. The UV–vis absorption spectra for CoPc using DMF as the solvent and the diffuse reflectance spectrum for CoPc/MCM-41 (dash dot) in the range 300–800 nm are shown in Fig. 2. CoPc exhibited two evident absorption bands at 327 nm (B band) and 657 nm (Q band), which correspond to the B band and Q band of phthalocyanines. Compared with the CoPc, CoPc/MCM-41 showed the absorption peak of CoPc at 698 nm, the bathochromic shift of the Q-band was due to the larger π structure in CoPc/MCM-41. Moreover, the absorption of dimer at 664 nm was quite obvious.

FT-IR spectra for CoPc, calcined MCM-41, and CoPc/MCM-41 were presented in Fig. 3, recorded in the fundamental region 400–4,000 cm^{-1} and used the KBr disk technique. The CoPc's spectrum showed absorption peaks around 731, 873, 949, 1,039, 1,092, and 1,122 cm^{-1} which may be assigned to phthalocyanine skeletal vibrations [27]. The vibrational bands of CoPc match well with the reported values for CoPc in the literature [28]. The spectrum also showed absorption peaks in the range around 3,060 cm^{-1} due to the aromatic C–H stretching as well as absorption bands around 1,480 cm^{-1}, assignable to C–C bonds. The FT-IR spectrum of CoPc/MCM-41 showed a few bands more than MCM-41, around 2,900 and 1,500 cm^{-1}, which were due to the aromatic C–H stretching. The result showed that the CoPc had been anchored to the walls of MCM-41. These observations clearly provide more evidences that CoPc is anchored to the calcined MCM-41.

The structural features of the MCM-41 before and after immobilization were checked by XRD measurements. The XRD of the loaded sample was also investigated. Fig. 4 shows that the patterns of the loaded samples are similar to that of the parent MCM-41 sample. However, slight differences in terms of both the positions and intensities of the first (1 0 0) peak were observed. Especially in loaded sample, the reflections are much weaker due to the presence of the guest species in the pores and occurrence of some disordering.

Fig. 5 displays the morphology of MCM-41 and CoPc/MCM-41. The SEM image (Fig. 5(a)) shows the random pore size distributions and interconnected

Table 1
Textural parameters for the supports and the catalyst

Sample	Surface area (m^2/g)	Pore volume (cm^3/g)	Pore size (Å)
MCM-41	1,060	0.97	36.61
CoPc/MCM-41	630	0.56	35.26

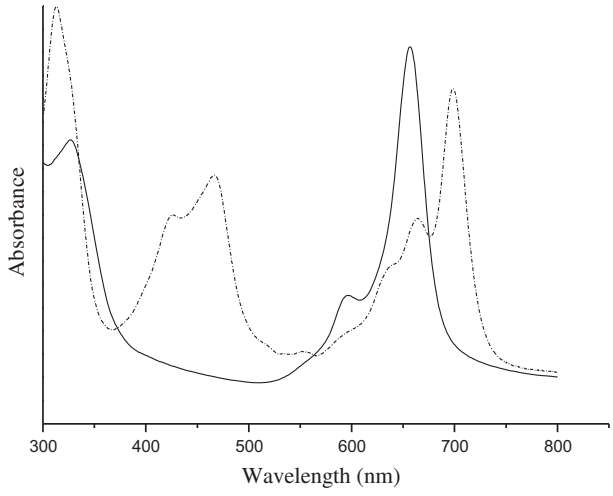

Fig. 2. UV–vis absorption spectra of CoPc (solid) and CoPc/MCM-41 (dash dot) in DMF solution.

pore systems in MCM-41. The surface morphology of the CoPc/MCM-41 (Fig. 5(b)) revealed by SEM image shows that the tight and brawny CoPc, which is observed clearly with the appearance of a stick-like morphology, is present in the CoPc/MCM-41.

3.2. Photocatalytic decomposition of methyl orange

3.2.1. The effect of visible light

Fig. 6 shows the degradation rate changes of methyl orange with time under various conditions. We could learn that the rate was 72.6% under visible light, which was much higher than that in dark condition (6%). Controlled experimental conditions indicate that the visible light is essential for efficient degradation of methyl orange in the irradiated aqueous solution, which was hardly degraded in the dark even in the presence of the catalyst.

3.2.2. The effect of immobilization

Our primary tests for degradation of methyl orange in Fig. 7 showed that when CoPc are being used, the rate of degradation is much less than when

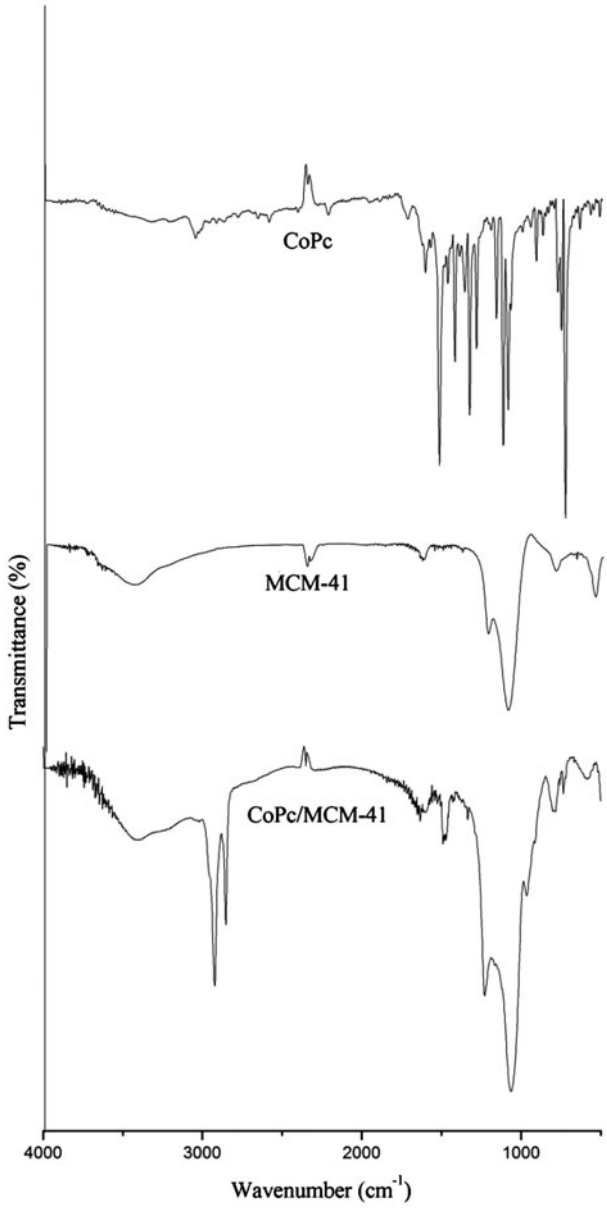

Fig. 3. FT-IR spectra of CoPc, calcined MCM-41, and CoPc/MCM-41.

CoPc supported MCM-41 was used. Actually, the later was about 20% higher than the former. It also showed

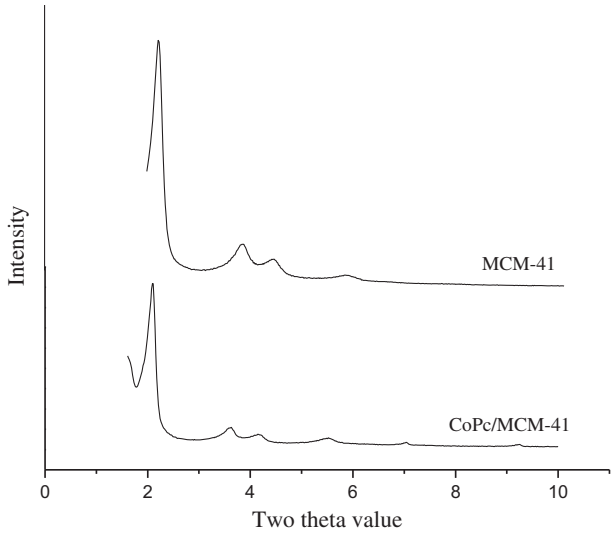

Fig. 4. Powder XRD patterns of calcined MCM-41 and CoPc/MCM-41.

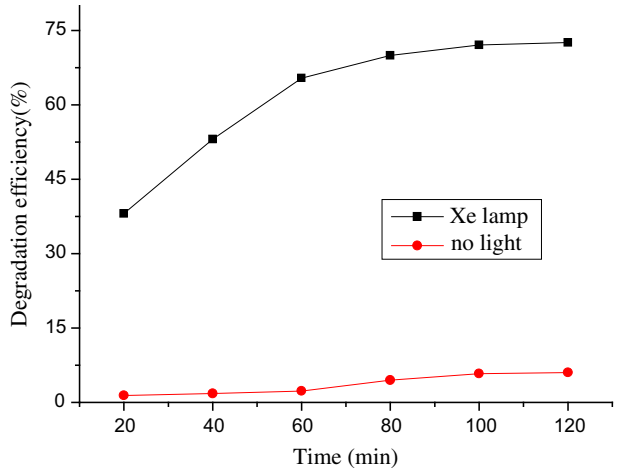

Fig. 6. Effect of visible light on the degradation of methyl orange. Irradiation source: xenon lamp, 200 mL methyl orange solution (0.05 g/L), 0.03 g catalyst.

that the support had hardly any catalytic activity after adsorbed and saturated. Catalyst immobilization onto MCM-41 has an enhancement effect in the degradation of methyl orange. This enhancement may be associated to two factors. On the one hand, MCM-41 has a regular honeycomb array of uniform cylindrical pores, which can be tailored to pore sizes ranging from 15 to 100 Å [29]. That means a large specific surface which increase contact area with methyl orange so as to accelerate the reaction rate; on the other hand, production and influence of dimeric species in solution are reduced in the presence of MCM-41. Because the dimeric species formed by coordination between water molecules and central atom of CoPc by hydrogen bond, the high absorptivity of MCM-41 was easy to separate for CoPc and weakened or even broken the hydrogen bond so that resulted in inhibiting the formation of dimeric species [30].

3.2.3. The effect of catalyst amount

The effect of the catalyst dose in suspension of methyl orange was investigated for an optimal condition was shown in Fig. 8. At low photocatalyst loading, the removal of the organic compound methyl orange increased linearly with the catalyst loading. However, both less and excess photocatalyst in the reaction solutions could impact the degradation rate of methyl orange dramatically. The catalyst was too little to react with all the organic compound, while the excess catalyst cause a shielding effect in penetration of light [31]. Above all, the degradation rate increased with increasing amount of the catalyst added within

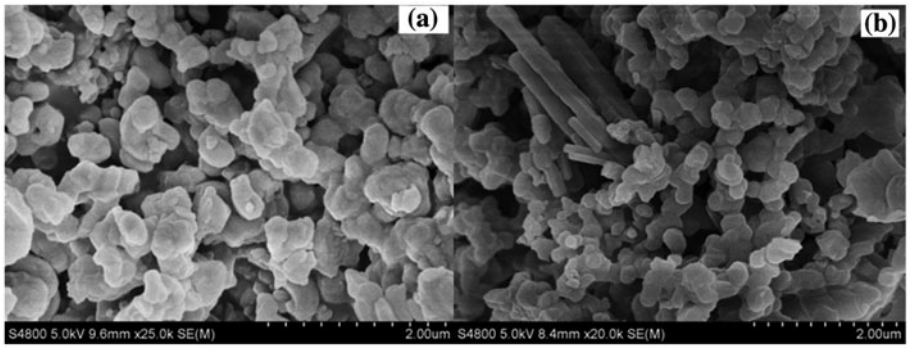

Fig. 5. SEM images of (a) MCM-41 and (b) CoPc/MCM-41.

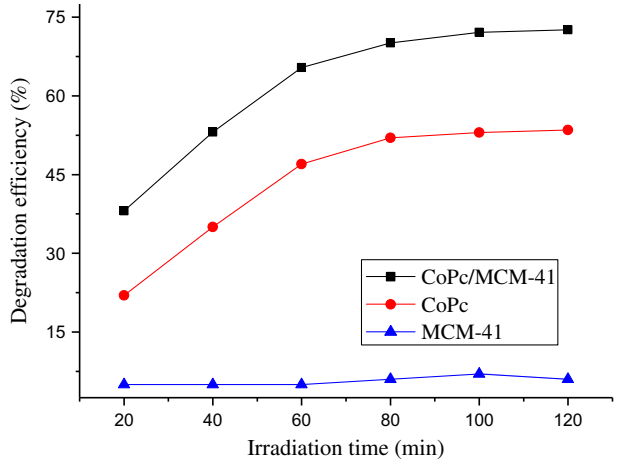

Fig. 7. Effect of immobilized catalyst on the degradation of methyl orange. Irradiation source: xenon lamp, 200 mL methyl orange solution (0.05 g/L), 0.03 g CoPc, 0.03 g MCM-41 or 0.03 g CoPc/MCM-41.

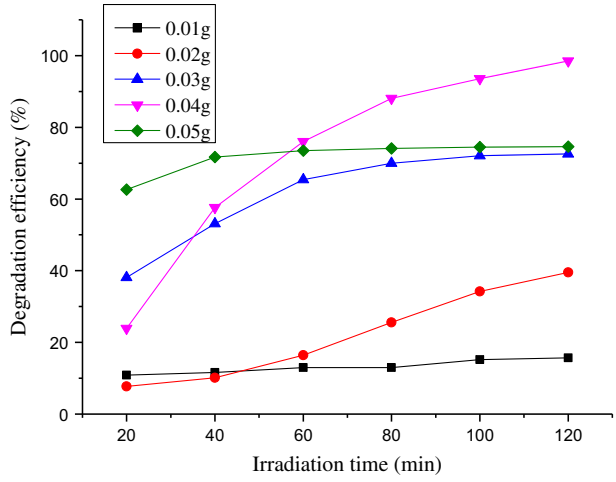

Fig. 8. Effect of visible light on the degradation of methyl orange. Irradiation source: xenon lamp, 200 mL methyl orange solution (0.05 g/L).

0.01 g–0.05 g/200 mL. The optimal catalyst amount is 0.04 g/200 mL for methyl orange degradation, and the degradation efficiency is 98.3%, which is much better than some semiconductors (Table 2).

The photodegradation process starts with the photogeneration of singlet oxygen and/or superoxide radicals by the immobilized phthalocyanine species anchored to the inner pore walls of MCM-41 upon irradiation. We attempted to verify which of these two radicals are involved in the photodegradation process through estimation of the yield of hydroxyl radicals. The hydroxyl radicals formation was checked using a procedure proposed by Gao et al. [39,40], based on Nash's method [41]. It is based on the quantification of the formaldehyde concentration formed during the oxidation of methanol by the hydroxyl radicals generated in the course of the photocatalytic process. We noticed that presence of hydroxyl radicals would produce a yellow color owing to the synthesis of diacetyldihydrolutidin [41]. We observed the color when our catalyst and the radiation were employed. The intensity of the color increased with increasing the time of radiation.

3.3. Catalyst reusability

The stability of the anchored catalysts is very important for its application in environmental technology. So, cyclic utilization is essential to evaluate a catalyst. Therefore, the effectiveness of catalyst reuse was

Table 2
Comparison between other inorganic catalysts and ours

Number	Catalyst	Optimal amount (g)	Light source (UV/vis)	Irradiation time (min)	Degradation efficiency (%)	Refs.
1	ZnO nanoglobules	0.2	UV	150	94.3	[32]
2	$BaTiO_3$@g-C_3N_4	0.5	Vis	360	77	[33]
3	$PbMoO_4$ and $PbWO_4$	0.1	UV	1,200	99	[34]
4	ZnO nanoneedles	0.2	UV	140	95.4	[35]
5	Sb_2S_3	0.1	Vis	120	98	[36]
6	MoS_2 nanosheets	0.5	Vis	70	100	[37]
7	CuO/zeolite X	0.1	UV	120	60	[38]
8	CoPc/MCM-41	0.04	Vis	120	98.3	Our work

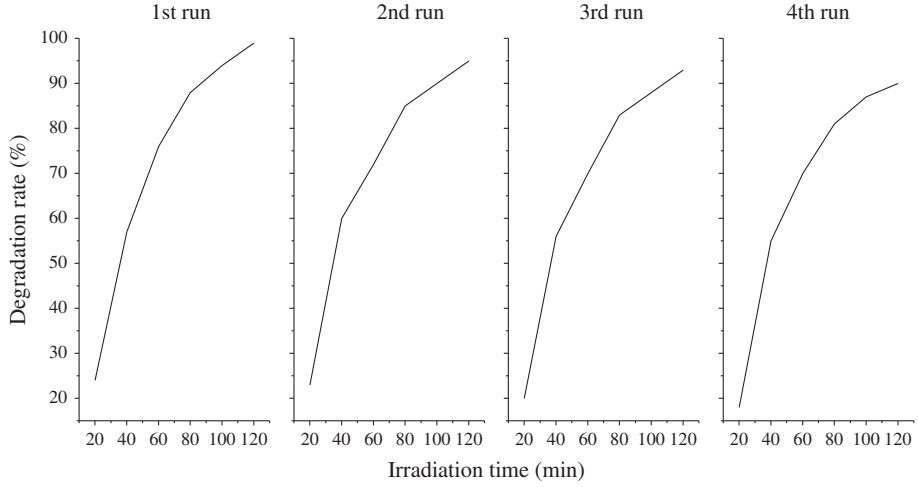

Fig. 9. Reuse of the CoPc/MCM-41 catalyst for methyl orange photodegradation for four successive cycles. 200 mL methyl orange (0.05 g/L), 0.04 g catalyst, and 120 min irradiation time under visible light irradiation.

examined for degradation of methyl orange during a four cycle experiment. Each experiment was carried out under identical conditions. After each experiment, the solution residue from the photocatalytic degradation was centrifuged, filtered, washed, and the solid was dried. The dried catalyst samples were used again for the degradation of methyl orange, employing similar experimental conditions [19]. The results were shown in Fig. 9. Recycling experiments showed a photocatalytic activity reduction from 99 to 90% of methyl orange degradation after four catalytic cycles. Possibly deactivation of the part of the catalyst surface, due to permanent adsorption of intermediate species, might be involved in reduction of its activity.

To test for CoPc leaching, we washed the dried recovered solid with DMF till the filtrate turned colorless, then dried and weighed. The difference between the two numbers was CoPc leaching, so the rate was about 8%. In fact the catalyst surface was observed to suffer a color change from dark blue to pale blue after the first photoreaction. Other possibility for the reduction of the activity of the catalyst could be due to probable attack of hydroxyl radicals to the anchored phthalocyanine complex.

4. Conclusions

The anchorage of CoPc in the channels of the calcined MCM-41 molecular sieves has been achieved by post-synthesis method. From the results described, it could be inferred that the visible light is essential for efficient degradation of methyl orange, and the catalyst immobilization onto MCM-41 has an enhancement effect in the degradation of methyl orange. The catalyst displays an efficient photoactivity for the degradation of methyl orange under visible light illumination. The photodegradation process is completed within 2 h for a concentration of 0.05 g/L of methyl orange and a dose of 0.04 g/L of the catalyst under visible light irradiation.

Acknowledgments

The authors would like to acknowledge the financial support from the National Science and Technology Major Project of the Ministry of Science and Technology of China (No. 2016ZX05040003). We also gratefully acknowledge the Research Department of China University of Petroleum (East China) for supporting this work.

References

[1] P.S. Mukherjee, A.K. Ray, Major challenges in the design of a large-scale photocatalytic reactor for water treatment, Chem. Eng. Technol. 22 (1999) 253–260.
[2] Z. Zhang, C. Shao, X. Li, C. Wang, M. Zhang, Y. Liu, Electrospun nanofibers of p-type NiO/n-type ZnO heterojunctions with enhanced photocatalytic activity, ACS Appl. Mater. Interfaces 2 (2010) 2915–2923.
[3] M.R. Hoffmann, S.T. Martin, W. Choi, D.W. Bahnemann, Environmental applications of semiconductor photocatalysis, Chem. Rev. 95 (1995) 69–96.
[4] G.K. Mor, O.K. Varghese, R.H.T. Wilke, S. Sharma, K. Shankar, T.J. Latempa, K.S. Choi, C.A. Grimes, p-Type Cu−Ti−O nanotube arrays and their use in self-biased heterojunction photoelectrochemical diodes for hydrogen generation, Nano Lett. 8 (2008) 1906–1911.

[5] M.A. Mahmood, S. Baruah, J. Dutta, Enhanced visible light photocatalysis by manganese doping or rapid crystallization with ZnO nanoparticles, Mater. Chem. Phys. 130 (2011) 531–535.
[6] L.B. Reutergådh, M. Iangphasuk, Photocatalytic decolourization of reactive azo dye: A comparison between TiO_2 and us photocatalysis, Chemosphere 35 (1997) 585–596.
[7] X.F. Wang, S. Zhan, Y. Wang, P. Wang, H.G. Yu, J.G. Yu, C.Z. Hu, Facile synthesis and enhanced visible-light photocatalytic activity of Ag_2S nanocrystal-sensitized $Ag_8W_4O_{16}$ nanorods, J. Colloid Interface Sci. 422 (2014) 30–37.
[8] C. Karunakaran, S. Kalaivani, P. Vinayagamoorthy, S. Dash, Electrical, optical and visible light-photocatalytic properties of monoclinic $BiVO_4$ nanoparticles synthesized hydrothermally at different pH, Mater. Sci. Semicond. Process. 21 (2014) 122–131.
[9] R. Asahi, T. Morikawa, T. Ohwaki, K. Aoki, Y. Taga, Visible-light photocatalysis in nitrogen-doped titanium oxides, Science 293 (2001) 269–271.
[10] C. An, S. Peng, Y. Sun, Facile synthesis of sunlight-driven AgCl:Ag plasmonic nanophotocatalyst, Adv. Mater. 22 (2010) 2570–2574.
[11] A. Kudo, K. Omori, H. Kato, A novel aqueous process for preparation of crystal form-controlled and highly crystalline $BiVO_4$ powder from layered vanadates at room temperature and its photocatalytic and photophysical properties, J. Am. Chem. Soc. 121 (1999) 11459–11467.
[12] J.B. Liu, Y. Zhao, F.S. Zhang, F.Q. Zhao, Y.W. Tang, X.Q. Song, G.Q. Yao, Dimerization of metal-free sulfonated phthalocyanines in aqueous methanol solution, Acta. Phys-Chim. Sin. 12 (1995) 163–168.
[13] V. Iliev, V. Alexiev, L. Bilyarska, Effect of metal phthalocyanine complex aggregation on the catalytic and photocatalytic oxidation of sulfur containing compounds, J. Mol. Catal. A: Chem. 137 (1999) 15–22.
[14] A.H. Sun, Z.G. Xiong, Y.M. Xu, Adsorption and photosensitized oxidation of sulfide ions on aluminum tetrasulfophthalocyanine-loaded anionic resin, J. Mol. Catal. A-Chem. 259 (2006) 1–6.
[15] Z.G. Xiong, Y.M. Xu, L.Z. Zhu, J.C. Zhao, Enhanced photodegradation of 2,4,6-trichlorophenol over palladium phthalocyaninesulfonate modified organobentonite, Langmuir 21 (2005) 10602–10607.
[16] R. Zugle, T. Nyokong, Zinc(II) 2,9,16,23-tetrakis[4-(N-methylpyridyloxy)]-phthalocyanine anchored on an electrospun polysulfone polymer fiber: Application for photosensitized conversion of methyl orange, J. Mol. Catal. A: Chem. 366 (2013) 247–253.
[17] B. Cojocaru, V.I. Parvulescu, E. Preda, G. Iepure, V. Somoghi, E. Carbonell, M. Alvaro, H. García, Sensitizers on inorganic carriers for decomposition of the chemical warfare agent yperite, Environ. Sci. Technol. 42 (2008) 4908–4913.
[18] A. Sanjuán, G. Aguirre, M. Alvaro, H. García, 2,4,6-Triphenylpyrylium ion encapsulated in Y zeolite as photocatalyst. A co-operative contribution of the zeolite host to the photodegradation of 4-chlorophenoxyacetic acid using solar light, Appl. Catal. B: Environ. 15 (1998) 247–257.
[19] M.A. Zanjanchi, A. Ebrahimian, M. Arvand, Sulphonated cobalt phthalocyanine–MCM-41: An active photocatalyst for degradation of 2,4-dichlorophenol, J. Hazard. Mater. 175 (2010) 992–1000.
[20] A. Corma, V. Fornes, H. Garcia, M.A. Miranda, M.J. Sabater, Highly efficient photoinduced electron transfer with 2,4,6-triphenylpyrylium cation incorporated inside extra large pore zeotype MCM-41, J. Am. Chem. Soc. 116 (1994) 9767–9768.
[21] P.A. Barrett, C.E. Dent, R.P. Linstead, Phthalocyanines. Part VII. Phthalocyanine as a coordinating group. A general investigation of the metallic derivatives, J. Chem. Soc. (Resumed) (1936) 1719–1736.
[22] M. Hu, Y. Xu, Z. Chen, Mineralization of 4-chlorophenol under visible light irradiation in the presence of aluminum and zinc phthalocyaninesulfonates, Chinese J. Chem. 21 (2003) 1092–1097.
[23] G.P. Cao, F. Xu, S.G. Xia, Preparation of a composite particle electrode by electroless plating and its electrocatalytic performance in the decolorization of methyl orange dye solution, J. Braz. Chem. Soc. 24 (2013) 2050–2058.
[24] H.P. Xia, M. Nogami, Copper phthalocyanine bonding with gel and their optical properties, Opt. Mater. 15 (2000) 93–98.
[25] A. Hadasch, A. Sorokin, A. Rabion, B. Meunier, Sequential addition of H_2O_2, pH and solvent effects as key factors in the oxidation of 2,4,6-trichlorophenol catalyzed by iron tetrasulfophthalocyanine, New J. Chem. 22 (1998) 45–51.
[26] W.X. Chen, B.Y. Zhao, Y. Pan, Y.Y. Yao, S.S. Lu, S.L. Chen, L.J. Du, Preparation of a thermosensitive cobalt phthalocyanine/N-isopropylacrylamide copolymer and its catalytic activity on thiol, J. Colloid Interface Sci. 300 (2006) 626–632.
[27] A.N. Sidorov, I.P. Kotlyar, Infrared spectra of phthalocyanines. I. The effect of crystalline structure and of the central metallic atom on the phthalocyanine molecule in the solid state, Opt. Spektrosk. 11 (1961) 92–100.
[28] Z.H. Zhao, J.M. Fan, M.M. Xie, Z.Z. Wang, Photo-catalytic reduction of carbon dioxide with in-situ synthesized $CoPc/TiO_2$ under visible light irradiation, J. Cleaner Prod. 17 (2009) 1025–1029.
[29] J.S. Beck, J.C. Vartuli, W.J. Roth, M.E. Leonowicz, C.T. Kresge, K.D. Schmitt, C.T.-W. Chu, D.H. Olson, E.W. Sheppard, S.B. McCullen, J.B. Higgins, J.L. Schlenker, A new family of mesoporous molecular sieves prepared with liquid crystal templates, J. Am. Chem. Soc. 114 (1992) 10834–10843.
[30] C.C. Leznoff, A.B.P. Lever, Phthalocyanines-Properties and Applications, vol. 1, VCH, New York, NY, 1989, p. XII.
[31] L. Wu, A. Li, G. Gao, Zh. Fei, Sh. Xu, Q. Zhang, Efficient photodegradation of 2,4-dichlorophenol in aqueous solution catalyzed by polydivinylbenzene-supported zinc phthalocyanine, J. Mol. Catal. A: Chem. 269 (2007) 183–189.
[32] R. Khan, M.S. Hassan, P. Uthirakumar, J.H. Yun, M.S. Khil, I.H. Lee, Facile synthesis of ZnO nanoglobules and its photocatalytic activity in the degradation of methyl orange dye under UV irradiation, Mater. Lett. 152 (2015) 163–165.
[33] T. Xian, H. Yang, L.J. Di, J.F. Dai, Enhanced photocatalytic activity of $BaTiO_3$@g-C_3N_4 for the degradation of methyl orange under simulated sunlight irradiation, J. Alloys Compd. 622 (2015) 1098–1104.

[34] Z.Y. Yu, C.N. Dong, R.Y. Qiu, L.J. Xu, A.H. Zheng, Photocatalytic degradation of methyl orange by $PbXO_4$ (X = Mo, W), J. Colloid Interface Sci. 438 (2015) 323–331.
[35] N. Tripathy, R. Ahmad, J.E. Song, H.A. Ko, Y.B. Hahn, G. Khang, Photocatalytic degradation of methyl orange dye by ZnO nanoneedle under UV irradiation, Mater. Lett. 136 (2014) 171–174.
[36] J.T. Tang, J.Y. Li, Y. Cheng, P. Huang, Q. Deng, Facile hydrothermal-carbonization preparation of carbon-modified Sb_2S_3 composites for photocatalytic degradation of methyl orange dyes, Vacuum 120 (2015) 96–100.
[37] W.H. Liu, Q.Z. Hu, F. Mo, J.J. Hu, Y. Feng, H.W. Tang, H.N. Ye, S.D. Miao, Photo-catalytic degradation of methyl orange under visible light by MoS_2 nanosheets produced by H_2SiO_3 exfoliation, J. Mol. Catal. A: Chem. 395 (2014) 322–328.
[38] A. Nezamzadeh-Ejhieh, M. Karimi-Shamsabadi, Comparison of photocatalytic efficiency of supported CuO onto micro and nano particles of zeolite X in photodecolorization of Methylene blue and Methyl orange aqueous mixture, Appl. Catal., A 477 (2014) 83–92.
[39] R. Gao, J. Stark, D.W. Bahnemann, J. Rabani, Quantum yields of hydroxyl radicals in illuminated TiO_2 nanocrystallite layers, J. Photochem. Photobiol., A 148 (2002) 387–391.
[40] A.E.H. Machado, M.D. Franca, V. Velani, G.A. Magnino, H.M.M. Velani, F.S. Freitas, P.S. Müller Jr., C. Sattler, M. Schmücker, Characterization and evaluation of the efficiency of TiO_2/zinc phthalocyanine nanocomposites as photocatalysts for wastewater treatment using solar irradiation, Int. J. Photoenergy 145–148 (2008) 1–12.
[41] T. Nash, The colorimetric estimation of formaldehyde by means of the Hantzsch reaction, Biochem. J. 55 (1953) 416–421.